

of very low latitude whistlers are located around the conjugate point in the Indian Ocean. Recent results suggest that the path of propagation, i.e. geomagnetic field lines connecting the conjugate points should lie in the ionosphere, and ducted or pro-longitudinal mode of propagation is more likely to occur^{18–20}. Studies are pursued and the results obtained will enhance the existing knowledge on the intricacies involved with low latitude whistlers.

1. Storey, L. R. O., An investigation of whistling atmospherics. *Philos. Trans. R. Soc. London, Ser. A*, 1953, **246**, 113–141.
2. Helliwell, R. A., *Whistlers and Related Ionospheric Phenomena*, Stanford University Press, Stanford, California, USA, 1965.
3. Carpenter, G. B., An FM technique for observation of VLF whistler-mode-propagation. Technical Report No. 3, Nonr-225(27), Technical Report No. 3412-2, AF-AFOSR-62-370, Radioscience Lab., Stanford Electronics Labs, Stanford University, California, USA, 1963.
4. Hayakawa, M. and Tanaka, Y., On the propagation of low latitude whistlers. *Rev. Geophys. Space Phys.*, 1978, **16**, 111–125.
5. Sazhin, S. S., Hayakawa, M. and Bullough, K., Whistler diagnostics of magnetospheric parameters: a review. *Ann. Geophys.*, 1992, **10**, 293.
6. Singh, B. and Hayakawa, M., Propagation modes of low and very-low-latitude whistlers. *J. Atmos. Sol.–Terr. Phys.*, 2001, **63**, 1133–1147.
7. Singh, R. P., Singh, R. L., Hamar, D. and Lichtenberger, J., Application of matched filtering to short whistlers recorded at low latitudes. *J. Atmos. Sol.–Terr. Phys.*, 2004, **66**, 407–413.
8. Cerisier, J. C., A theoretical and experimental study of non-ducted VLF waves after propagation through the magnetosphere. *J. Atmos. Terr. Phys.*, 1973, **35**, 74.
9. Hayakawa, M., Tanaka, Y. and Ohta, K., Absolute intensity of low latitude whistlers as deduced from the direction finding measurements. *Radio Sci.*, 1985, **20**, 985.
10. Ondoh, T., Kotaki, M., Murakami, T., Watanabe, S. and Nakamura, Y., Propagation characteristics of low latitude whistlers. *J. Geophys. Res.*, 1979, **84**, 2099–2104.
11. Singh, B. and Tantry, B. A. P., On ducting of whistlers at low latitudes. *Ann. Geophys.*, 1973, **29**, 561–568.
12. Hayakawa, M. and Iwai, A., Magnetospheric ducting of low latitude whistlers as deduced from the rocket measurements of wave-normal direction. *J. Atmos. Terr. Phys.*, 1975, **37**, 1211.
13. Tanaka, Y. and Hayakawa, M., The effect of geomagnetic disturbance on duct propagation of low latitude whistlers. *J. Atmos., Terr. Phys.*, 1973, **35**, 1699–1703.
14. Tanaka, Y. and Cairo, L., Propagation of VLF waves through the equatorial anomaly. *Ann. Geophys.*, 1980, **36**, 555–575.
15. Andrews, M. K., Non-ducted whistler mode signals at low latitudes. *J. Atmos. Terr. Phys.*, 1978, **42**, 1–20.
16. Thomson, N. R., Ray-tracing the paths of very low latitude whistler-mode signals. *J. Atmos. Terr. Phys.*, 1987, **49**, 321–338.
17. Kumar, S., Anil, D., Kishore, A. and Ramachandran, V., Whistlers observed at low-latitude ground-based VLF facility in Fiji. *J. Atmos. Sol.–Terr. Phys.*, 2007, **69**, 1366–1376.
18. Singh, R. *et al.*, Very low latitude ($L = 1.08$) whistlers. *Geophys. Res. Lett.*, 2012; doi:10.1029/2012GL054122.
19. Srivastava, P. R. *et al.*, One to one relationship between low latitude whistlers and conjugate source lightning discharges and their propagation characteristics. *J. Adv. Space Res.*, 2013, **52**, 1966–1973.
20. Gokani, S. A. *et al.*, Very low latitude ($L = 1.08$) whistlers and correlation with lightning activity. *J. Geophys. Res. Space Phys.*, 2015, **119**; doi:10.1002/2015JA021058.
21. Collier, A. B., Bremner, S., Lichtenberger, J., Downs, J. R., Rodger, C. J., Steinbach, P. and McDowell, G., Global lightning distribution and whistlers observed at Dunedin, New Zealand. *Ann. Geophys.*, 2010, **28**(2), 499–513.
22. Rodger, C. J., Brundell, J. B. and Holzworth, R. H., Improvements in the WWLLN network: bigger detection efficiencies through more stations and smarter algorithms. In Paper presented at the 11th Scientific Assembly, International Association of Geomagnetism and Aeronomy, Sopron, Hungary, 2009.
23. Singh, R. *et al.*, Initial results from AWESOME VLF receivers: set up in low latitude Indian regions under IHY2007/UNBSSI program. *Curr. Sci.*, 2010, **98**(3), 398–405.
24. Lichtenberger, J., Ferencz, C., Bodnár, L., Hamar, D. and Steinbach, P., Automatic whistler detector and analyser system: automatic whistler detector. *J. Geophys. Res.*, 2008, **113**, A12201; doi:10.1029/2008JA013467.
25. Wood, T. G., Geo-location of individual lightning discharges using impulsive VLF electromagnetic waveforms. Ph D theses, Stanford University, California, USA, 2005.
26. Said, R. K., Accurate and efficient long range lightning geo-location using a VLF radio atmospheric waveform bank, Ph D theses, Stanford University, California, USA, 2009.

ACKNOWLEDGEMENTS. We thank the Director, Indian Institute of Geomagnetism (IIG), Navi Mumbai, for support and encouragement. The whistler data used in the present study are taken from the IIG (<http://iigm.res.in/>) operated VLF stations in India. We also thank Robert Holzworth, University of Washington, USA (bobholz@ess.washington.edu) for providing WWLLN data (<http://webflash.ess.washington.edu/>), and the International Space Weather Initiative Program and United Nations Basic Space Sciences Initiative programme for their support to VLF project activities in India.

Received 7 December 2015; revised accepted 15 February 2016

doi: 10.18520/cs/v111/i1/198-201

A synoptic-scale perspective of heavy rainfall over Chennai in November 2015

A. Chakraborty*

Centre for Atmospheric and Oceanic Sciences and Divecha Centre for Climate Change, Indian Institute of Science, Bengaluru 560 012, India

The South Indian city of Chennai experienced three phases of heavy rainfall that resulted in devastating flood during November and early December of 2015. We find that propagating convective systems from the west Pacific Ocean intensified further over the warm Indian Ocean before moving north towards Indian land region. This northward propagation was guided by two highs of mid-troposphere to the east and west

*e-mail: arch@caos.iisc.ernet.in

of the Indian region. While the high to the east was typical of an El Niño year, that the west was associated with global phase shift of upper tropospheric Rossby wave. Similar highs to the west were present during other years of heavy rainfall along the east coast of peninsular India.

Keywords: Convective systems, floods, heavy rainfall, monsoon.

EXTREME weather events are on the rise around the world during the past few decades^{1–4}. This includes frequent occurrences of extreme temperature^{5–8} and rainfall^{1–3,9–11} and increase in tropical cyclone intensity^{12–15}. The frequency of occurrence of extreme rain events over the Indian land region in summer monsoon season has increased during the past six decades¹⁶. This increase in synoptic-scale convection is partially compensated by a decrease in the intensity of the slowly-varying component of the monsoon intraseasonal oscillation (ISO)¹⁷, which has resulted in a relatively insignificant change in its seasonal mean¹⁶.

During October–December, the intertropical convergence zone (ITCZ) located near the equator and southeastern parts of peninsular India, and lower tropospheric winds blow from northeast over the Bay of Bengal and bring moisture to the east coast of peninsular India. These three months (October–December) contribute 12% of the annual rainfall all over India (143 out of annual 1159 mm over land parts of 70–90°E, 8–28°N). Many meteorological subdivisions of South India receive 17%–49% of annual rainfall in this season^{18,19}. Tamil Nadu receives the highest seasonal rainfall during this northeast monsoon season (October–November). Sreekala *et al.*¹⁹ have shown that the interannual variation of intensity of the northeast monsoon over India is large. This is related to sea-surface temperature (SST) of equatorial Pacific and Indian Oceans^{19,20}. Some of these interannual variations in seasonal mean occur due to few heavy rainfall events. One such heavy event was observed over the southeast peninsular India during November 2015 that resulted in unprecedented flooding in the city of Chennai. In this communication, using available satellite based rainfall and reanalysis datasets, we analyse the synoptic situations associated with these extreme rainfall events to explain their location, duration and intensity.

Rainfall climatology of November for the period 1998–2014 from Tropical Rainfall Measurement Mission (TRMM 3B42)-based estimates (Figure 1a) shows the ITCZ, defined as the location of intense rainfall, situated over the eastern equatorial Indian Ocean. A region off the east coast of the Indian peninsula also receives heavy rainfall (> 9 mm/day) during this month. This is the typical spatial pattern of the northeast monsoon. Figure 1b shows rainfall in November 2015 over the same domain, estimated from multiple satellites under the Global Pre-

cipitation Measurement (GPM) project. Intense rain band exceeding 24 mm/day along the southeast coast of the Indian peninsula was experienced during this month. It is also evident that rainfall over the equatorial Indian Ocean in November 2015 was higher compared to the TRMM climatology. The rich spatial structure in GPM (Figure 1b), compared to that in TRMM (Figure 1a, 0.25 × 0.25 degrees), can be attributed to higher spatial resolution of the GPM (0.1 × 0.1 degrees), as well as long-term averaging of the TRMM datasets.

Figure 2 shows the daily time series of rainfall over three 2 × 2 degree regions in and around Chennai. There were three episodes of heavy rainfall in November and early December of 2015, which contributed to the high monthly mean intensity seen in Figure 1b. It is evident from the time lag in the occurrences of peaks over these three regions (the southernmost box experienced heavy rainfall first, followed by the middle and northern boxes), that these convective systems moved from south to north along the east coast of the Indian peninsula. The third system, which occurred during 29 November–3 December 2015, did not produce heavy rainfall over the northern box (north of Chennai). The region around Chennai (represented by the red-coloured curve in Figure 2) experienced 71% of the total rainfall from 1 November to 4 December 2015 during these three 3-day long events (7–9 November, 14–16 November and 30 November–2 December).

The aforementioned northward propagation is evident from Figure 3a which shows a time–latitude plot of rainfall averaged between 79°E and 82°E. During November 2015, two northward-propagating systems moved from near the equator to about 15°N along the east coast of peninsular India. This resulted in time-delayed peak in rainfall rate over the three regions shown in Figure 2. The third system was initially weaker compared to the first two, consistent with the time series. This finally gained strength on 30 November 2015. Figure 3b shows that the westward propagation was prominent along 5–8°N latitude over south Bay of Bengal. Note that the day of appearance of these westward-propagating systems at around 80°E was coincidental with the northward-propagating systems along the same location (guided by bold lines in the figure for the first two events). Therefore, it appears that the westward-propagating convections merged with or turned into northward-propagating systems along 80°E.

Figure 4 shows the geopotential height (GPH) of 500 hPa pressure level before, during and after these three phases of heavy rainfall events (from NCEP/NCAR reanalysis dataset²¹; 8–10 November, 14–16 November and 30 November–2 December of 2015). A high (low) value of GPH signifies high (low) pressure. Horizontal winds, which are generally in quasi-geostrophic balance, blow in a clockwise (anticlockwise) direction around a high (low) GPH region. The cyclonic circulations at the southern tip of India identify these convective systems. On 8 November 2015, when the low-pressure system was

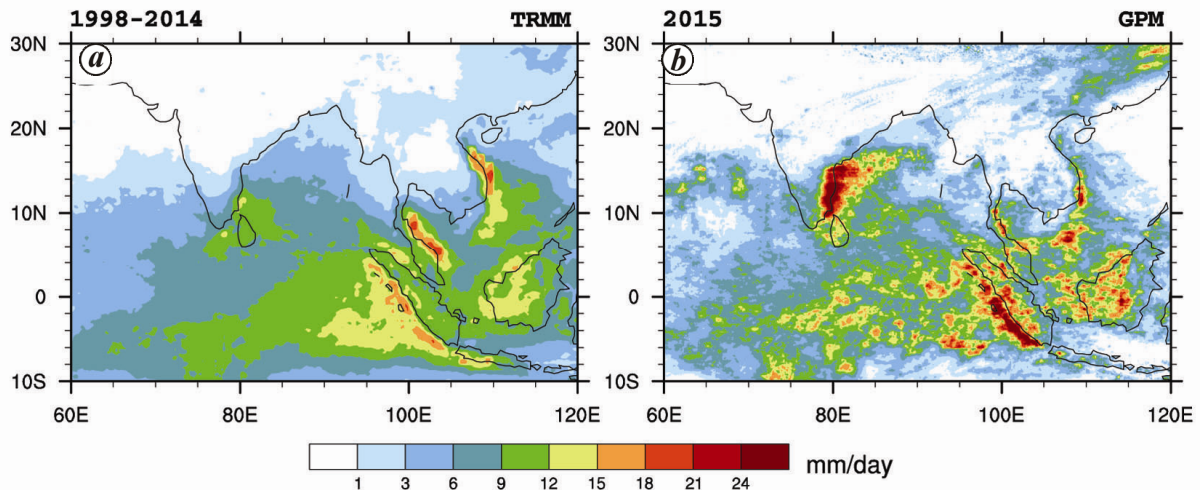


Figure 1. Rain rate (mm/day) in November. *a*, 1998–2014 climatology from TRMM 3B42 dataset. *b*, As estimated by GPM for November 2015.

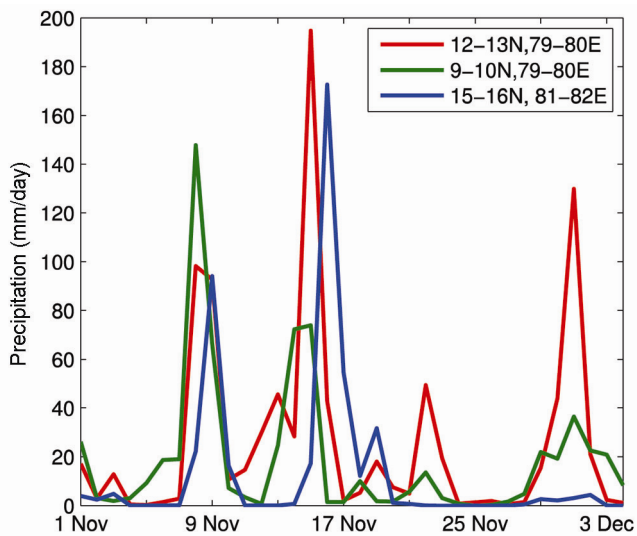


Figure 2. Daily time series of rainfall rate over three 2×2 degree regions over and around Chennai during 1 November to 4 December 2015.

centred at 80°E , 10°N (Figure 4*a*), two highs were pronounced at around 20°N , east and west of this low. On 9 November when the low pressure intensified, the high GPH region to the west moved further east, with its eastern edge intensifying further. On 10 November this high moved further east while the peninsular low weakened. Similar synoptic conditions of two highs to the east and west of the Indian region can be noticed during the other heavy rainfall episodes (Figure 4*d–f*). It is argued here that the trapping of the low-pressure systems between two strong high GPH systems in the east and west did not allow the convection to move in these directions. It then moved more or less northward along the east coast of peninsular India (Figure 3*a*).

These zonally propagating waves, identified in the GPH field in Figure 4, are illustrated in Figure 5 as time–longitude cross-sections. At 200 hPa along $25\text{--}30^\circ\text{N}$ (Figure 5*a*), alternate highs and lows move eastward at a speed of about 6 m/s. These are upper tropospheric Rossby waves, seen at the southern flank of the jet stream, that originated because of meridional perturbation of wind field due to earth's rotation²². Breaking of blocking highs over western Asia generates some of these westward-propagating waves. Propagation of such highs closer to Indian region results in advection of dry desert air toward Indian land and intensifies break phase of the summer monsoon²³. In Figure 5*b*, much closer to the equator along $10\text{--}15^\circ\text{N}$, in the middle troposphere (500 hPa), the propagation is predominantly to the west direction^{24,25}. Speed of these westward-propagating synoptic systems is 4–5 times more than the eastward-propagating Rossby waves of the northern latitudes. These westward-propagating waves are also seen in surface pressure and velocity potential fields^{24,25}. The vertical solid lines in Figure 5 show the approximate location of Chennai (80°E). The horizontal solid lines are days of maximum rainfall (according to time series of Figure 2). Note that in all the three phases, when rainfall rate is highest, the convective system is between two highs of the 200 hPa Rossby wave. This is also evident from Figure 3*a*, showing that the convective systems are generated near the equator and propagate-northward, before getting trapped between the high-pressure systems east and west of Indian region.

To check if the appearance of two highs in GPH to the east and west of the Indian region is common during other El Niño years, we plotted the El Niño composites of 500 hPa GPH in November for the period 1948–2014 (Figure 6*a*). We consider a year to be an El Niño year when the Niño 3.4 SST anomaly (obtained from

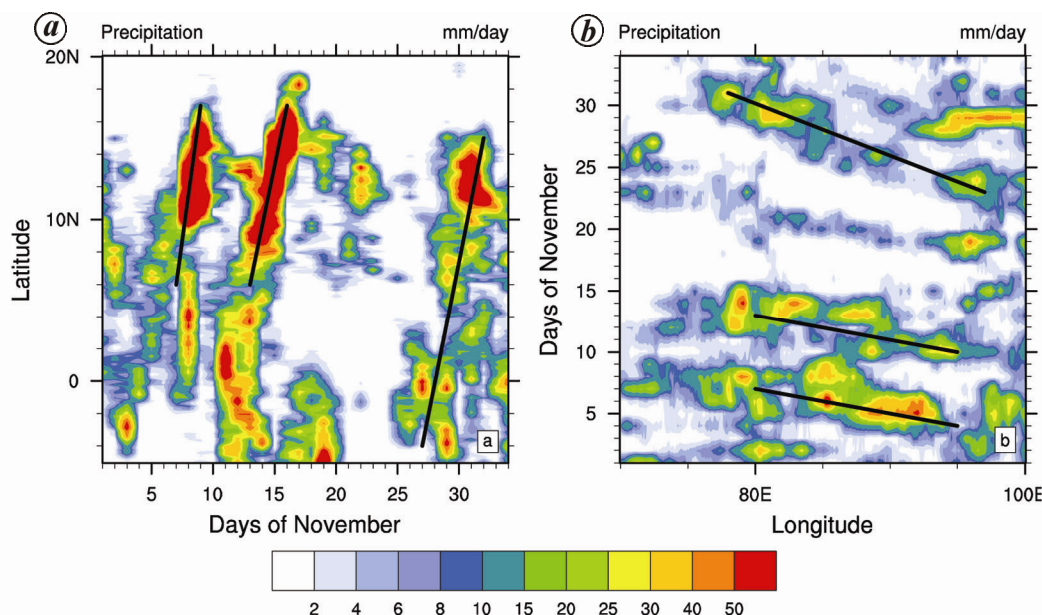


Figure 3. Time–latitude cross-section along 79–82°E (a), and time–longitude cross-section along 5–8°N (b), for rainfall during 1 November to 4 December 2015, estimated by GPM satellites.

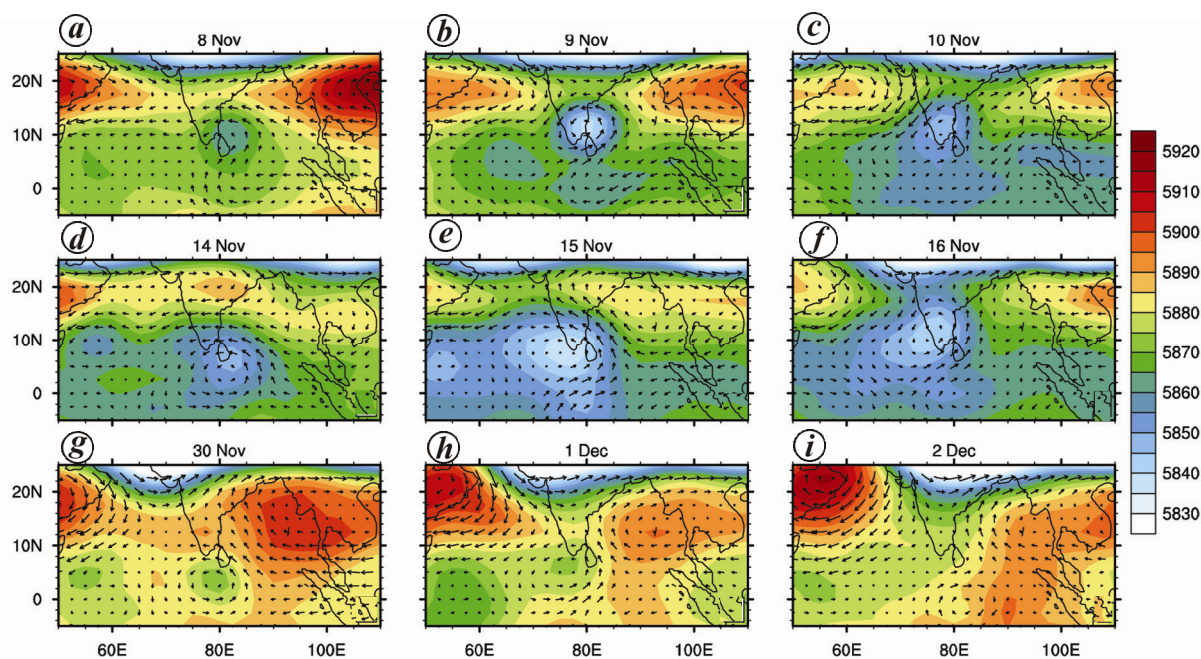


Figure 4. Geopotential height of 500 hPa pressure level before, during and after the three phases of heavy rainfall along the southeast coast of the Indian peninsula during November–December 2015. The horizontal wind vectors of the pressure level are also shown.

HadISST²⁶) in November of that year is above +1°C. Figure 6a suggests an anomalous high over the Bay of Bengal (east of the Indian land region) during El Niño years. However, to the west over Middle East and Saudi Arabia, a low at 500 hPa is prominent in this composite. In November 2015, the high of the east moved further north and the low of Arabia was replaced by a high (Figure 6b). This Arabian high, extending further east

towards the Indian region was responsible for restricting the convective systems to move further west in November 2015.

An obvious question arises: did similar intense rainfall occur over South India in other years with two highs in GPH to its east and west? Table 1 shows a list of intense rainfall events recorded in November since 1948 over the east coast of peninsular India. A composite of 500 hPa

Table 1. List of heavy rainfall events along the east coast of peninsular India during November from 1948 to 2014 (the period for which reanalysis data are available)

Location	Longitude, latitude (°)	Date	Intensity (cm)
Annamalai, Tamil Nadu	79.71, 11.39	20 November 1959	52
Mahabalipuram, Tamil Nadu	80.19, 12.61	20 November 1970	54
Meenambakkam, Tamil Nadu	80.17, 12.98	25 November 1976	35
Cuddalore, Tamil Nadu	79.75, 11.75	4 November 1978	38
Karaikal, Tamil Nadu	79.83, 10.93	15 November 1991	48
Orathanadu, Tamil Nadu	79.25, 10.62	27 November 2008	66
Thanjavur, Tamil Nadu	79.13, 10.78	27 November 2008	53
Vedaranniyam, Tamil Nadu	79.85, 10.37	27 November 2008 </td <td>42</td>	42

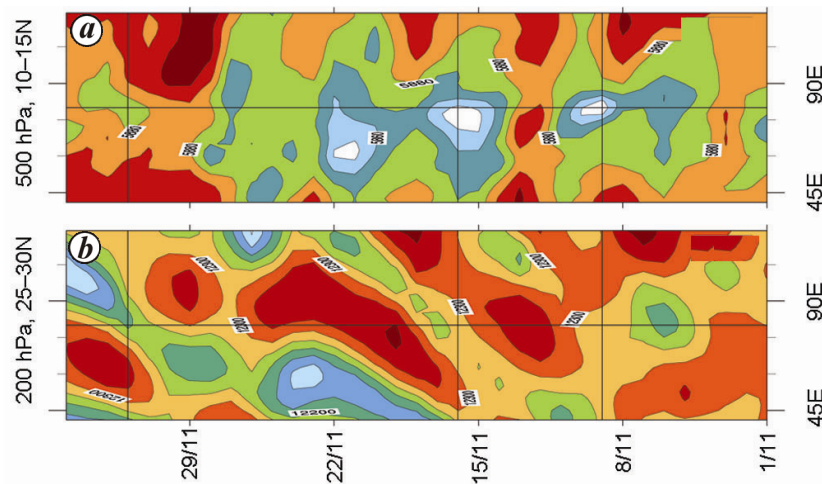


Figure 5. Time-longitude cross-section of geopotential height along (a) 25–30°N for 200 hPa and (b) 10–15°N for 500 hPa, obtained from NCEP/NCAR reanalysis dataset.

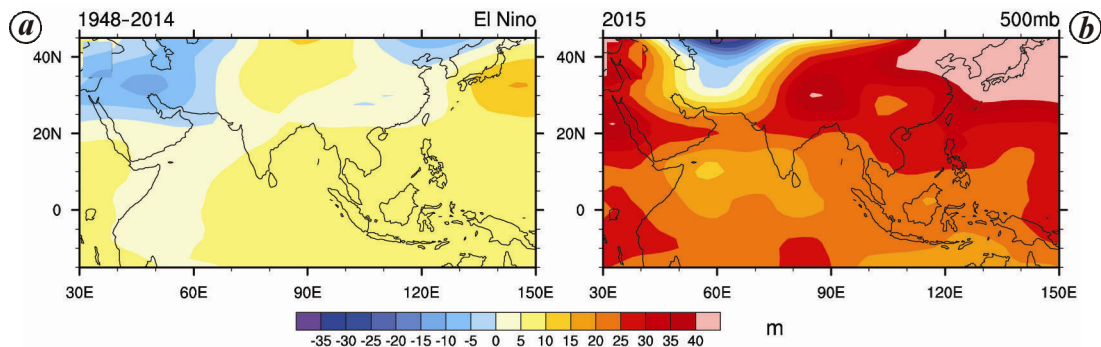


Figure 6. a, El Niño year composite of geopotential height of 500 hPa during November 1948 through 2014. b, Geopotential height anomaly of 500 hPa in November 2015.

GPH of these days (Figure 7) shows the circular low-pressure system near the east coast of southern India. Also noticeable are the two high GPH systems to the east and west of the Indian region. This spatial pattern of GPH is similar to that shown in Figure 4 that occurred during heavy rainfall events of November 2015.

Figure 8 shows the spatial variation of linear correlation coefficient between monthly mean rainfall (derived

from the India Meteorological Department rain gauge measurements and interpolated to 1×1 degree grids)²⁷ all over the Indian land region and area-averaged 500 hPa GPH over 30–60°E, 20–45°N in November for the period 1948–2014. This region for GPH was chosen considering the synoptic conditions in Figure 4. Figure 8 suggests that a high GPH over Middle East is positively correlated with high amount of rainfall over central and south Indian

land regions. Note also that the highest positive correlation is found along the east coast of the Indian peninsula over Tamil Nadu and Andhra Pradesh. Combining this with Figures 4 and 7, we can conclude that an anomalous mid-tropospheric high to the west of the Indian region can induce anomalous northerly to the north that does not allow propagating systems to move further north and west. This results in dry conditions in the northwest Indian region and wet conditions to the southeast Indian peninsula. It suggests that an anomalous high over Middle East in November can help increase the northeast monsoon rainfall over South India.

In summary, this communication analyses the synoptic conditions associated with heavy rainfall events over the east coast of peninsular India during November–early December of 2015 that caused devastating floods in Chennai. We find that the location of these convective systems is determined by circulation associated with two mid-tropospheric highs in geopotential to the east and

west sides of the Indian region. We also found that several events of heavy rainfall along the southeastern coast of peninsular India in the past did co-occur with similar highs in 500 hPa geopotential field to the west of the Indian region. It is possible that the intensity of rainfall rate was associated with increased moist static energy of lower troposphere that can destabilize the atmosphere on account of increase in SST of the Indian Ocean partially induced by El Niño (not shown)^{26–30}. While the hypothesis presented here needs to be tested with numerical model simulations in a future study, the proposition could be useful to diagnose the cause of errors in short-to-medium range forecasting of such events.

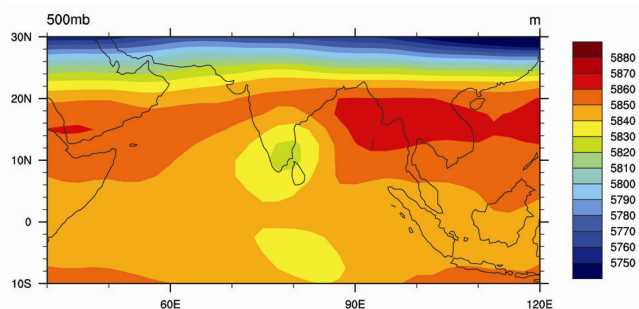


Figure 7. Composite of 500 hPa geopotential height during days of intense rainfall (listed in Table 1) along the east coast of India.

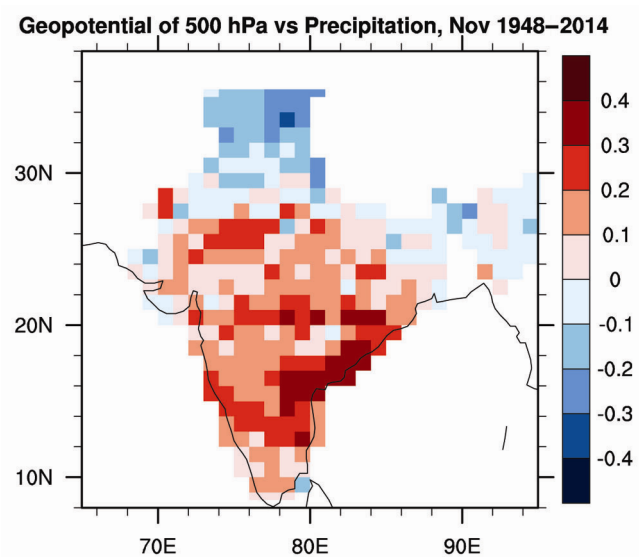


Figure 8. Correlation between time series of area-averaged geopotential height of 500 hPa over 30–60°E, 20–45°N, and rainfall over the Indian land region during November 1948 to 2014.

1. Kunkel, K., Andsager, K. and Easterling, D., Long-term trends in extreme precipitation events over the conterminous United States and Canada. *J. Climate*, 1999, **12**, 2515–2527.
2. Durman, C. F., Gregory, J. M., Hassell, D. C., Jones, R. G. and Murphy, J. M., A comparison of extreme European daily precipitation simulated by a global and a regional climate model for present and future climates. *Q. J. R. Meteorol. Soc.*, 2001, **127**, 1005–1015.
3. Wang, Y. and Zhou, L., Observed trends in extreme precipitation events in China during 1961–2001 and the associated changes in large-scale circulation. *Geophys. Res. Lett.*, 2005, **32**, 1–4.
4. Kharin, V. V., Zwiers, F. W., Zhang, X. and Wehner, M., Changes in temperature and precipitation extremes in the CMIP5 ensemble. *Climatic Change*, 2013, **119**, 345–357.
5. Karl, R., Change, J. and Ouayle, G., Global warming: Evidence for asymmetric diurnal temperature change. *Geophys. Res. Lett.*, 1991, **18**, 2253–2256.
6. Beniston, M. and Stephenson, D. B., Extreme climatic events and their evolution under changing climatic conditions. *Global Planet. Change*, 2004, **44**, 1–9.
7. Griffiths, G. M. *et al.*, Change in mean temperature as a predictor of extreme temperature change in the Asia-Pacific region. *Int. J. Climatol.*, 2005, **25**, 1301–1330.
8. Dash, S. K., Jenamani, R. K., Kalsi, S. R. and Panda, S. K., Some evidence of climate change in twentieth-century India. *Climatic Change*, 2007, **85**, 299–321.
9. Cavazos, T., Large-scale circulation anomalies conducive to extreme precipitation events and derivation of daily rainfall in north-eastern Mexico and southeastern Texas. *J. Climate*, 1999, **12**, 1506–1523.
10. Emori, S., Dynamic and thermodynamic changes in mean and extreme precipitation under changed climate. *Geophys. Res. Lett.*, 2005, **32**, L17706.
11. Pendergrass, A. G., Lehner, F., Sanderson, B. M. and Xu, Y., Does extreme precipitation intensity depend on the emissions scenario? *Geophys. Res. Lett.*, 2015, **42**, 8767–8774.
12. Emanuel, K., Increasing destructiveness of tropical cyclones over the past 30 years. *Nature*, 2005, **436**, 686–688.
13. Webster, P. J., Holland, G. J., Curry, J. A. and Chang, H. R., Changes in tropical cyclone number, duration, and intensity in a warming environment. *Science*, 2005, **309**, 1844–1846.
14. Knutson, T. R. *et al.*, Tropical cyclones and climate change. *Nature Geosci.*, 2010, **3**, 157–163.
15. Wing, A. A., Emanuel, K. and Solomon, S., On the factors affecting trends and variability in tropical cyclone potential intensity. *Geophys. Res. Lett.*, 2015, **42**, 8669–8677.
16. Goswami, B. N., Venugopal, V., Sengupta, D., Madhusoodanan, M. S. and Xavier, P. K., Increasing trend of extreme rain events over India in a warming environment. *Science*, 2006, **314**, 1442–1445.

17. Karmakar, N., Chakraborty, A. and Nanjundiah, R. S., Decreasing intensity of monsoon low-frequency intraseasonal variability over India. *Environ. Res. Lett.*, 2015, **10**, 054018.
18. Sontakke, N., Singh, N. and Singh, H., Instrumental period rainfall series of the Indian region (AD 1813–2005): revised reconstruction, update and analysis. *Holocene*, 2008, **18**, 1055–1066.
19. Sreekala, P. P., Rao, S. V. B. and Rajeevan, M., Northeast monsoon rainfall variability over south peninsular India and its teleconnections. *Theor. Appl. Climatol.*, 2012, **108**, 73–83.
20. Yadav, R. K., Emerging role of Indian ocean on Indian northeast monsoon. *Climate Dyn.*, 2013, **41**, 105–116.
21. Kalnay, E. *et al.*, The NCEP/NCAR 40-year reanalysis project. *Bull. Am. Meteorol. Soc.*, 1996, **77**, 437–471.
22. Hoskins, B. J. and Ambrizzi, T., Rossby wave propagation on a realistic longitudinally varying flow. *J. Atmos. Sci.*, 1993, **50**, 1661–1671.
23. Krishnamurti, T. N., Thomas, A., Simon, A. and Kumar, V., Desert air incursions, an overlooked aspect, for the dry spells of the Indian summer monsoon. *J. Atmos. Sci.*, 2010, **67**, 3423–3441.
24. Krishnamurti, T. N. and Ardanuy, P., The 10 to 20-day westward propagating mode and ‘breaks in the monsoon’. *Tellus A*, 1980, **32**, 15–26.
25. Chen, T.-C. and Chen, J.-M., The 1020-day mode of the 1979 Indian monsoon: its relation with the time variation of monsoon rainfall. *Mon. Weather Rev.*, 1993, **121**, 2465–2482.
26. Rayner, N. A. *et al.*, Global analyses of sea surface temperature, sea ice, and night marine air temperature since the late nineteenth century. *J. Geophys. Res.*, 2003, **108**, 4407.
27. Rajeevan, M., Bhatte, J., Kale, J. D. and Lal, B., Development of a high resolution daily gridded rainfall dataset for the Indian region. *Curr. Sci.*, 2006, **91**, 296–306.
28. Chakraborty, A., Nanjundiah, R. S. and Srinivasan, J., Theoretical aspects of the onset of Indian summer monsoon from perturbed orography simulations in a GCM. *Ann. Geophys.*, 2006, **24**, 2075–2089.
29. Chakraborty, A., Nanjundiah, R. S. and Srinivasan, J., Local and remote impacts of direct aerosol forcing on Asian monsoon. *Int. J. Climatol.*, 2014, **34**, 2108–2121.
30. Chakraborty, A., Satheesh, S. K., Nanjundiah, R. S. and Srinivasan, J., Impact of absorbing aerosols on the simulation of climate over the Indian region in an atmospheric general circulation model. *Ann. Geophys.*, 2004, **22**(5), 1421–1434.

ACKNOWLEDGEMENTS This work is supported by MoES/National Monsoon Mission and MoES/CTCZ programmes. I thank Md Tabrez Alam and Anirban Banerjee for help during data analysis. I also thank three reviewers and the editor for useful comments that helped improve the manuscript.

Received 25 December 2015; revised accepted 27 February 2016

doi: 10.18520/cs/v111/i1/201-207

Impact of temporal change of land use and cropping system on some soil properties in northwestern parts of Indo-Gangetic Plain

Jaya N. Surya^{1,*}, G. S. Sidhu¹, Tarsem Lal¹, D. K. Katiyar¹ and Dipak Sarkar²

¹ICAR-National Bureau of Soil Survey and Land Use Planning, Regional Centre Delhi, IARI Campus, New Delhi 110 012, India

²ICAR-National Bureau of Soil Survey and Land Use Planning, Amravati Road, Nagpur 440 033, India

Soil series representing different physiographic units were studied to know the impact of temporal change in land use and cropping system on some soil properties in the northwestern parts of the Indo-Gangetic Plain. The dynamics in land use and cropping system for the period 1983–84, 1996–97 and 2007–2008 and change in soil properties for the period 1983 and 2008 were studied. In Singhpur soil series developed on Shiwalik hills, the soil organic carbon (SOC) content decreased from 0.69% in 1983 to 0.40% in 2008 on account of increased deforestation and soil erosion. However, no significant changes were observed in soil pH and electrical conductivity (EC). In Manjuwal (upper piedmont plain) and Mandiani series (lower piedmonts) slight changes in SOC, pH, EC and calcium carbonate were found. In Naura series (normal soils), occurring in the old flood plain, SOC content of surface soils increased to >1.0% in 2008 compared to 0.41% in 1983 because of shifting of cropping system of maize–wheat to high biomass-producing cropping system (rice–wheat, rice–potato/mustard/peas/sunflower) and addition of fertilizers under high management practices. The soil pH and EC decreased slightly during 1983 to 2008. Similar results were also observed in Bhaura series (salt-affected soils) and Bairsal series in recent flood plains. Thus, the land use and cropping system in less-intensive cultivated areas of Shiwalik hills and piedmonts do not have much influence on the soil properties. However, in intensively cultivated areas of old and recent flood plains, where high biomass-producing rice–wheat system replaced wheat–maize system, the soil properties had changed to a large extent.

Keywords: Land-use dynamics, physiographic units, rice–wheat cropping system, soil quality parameters.

IN the northwestern parts of the Indo-Gangetic Plains, maize–wheat and cotton–wheat cropping systems were prevalent before the green revolution. After the green revolution era, particularly during the last 3–4 decades (from 1980 to 2010) rice–wheat cropping system became dominant in this region. This system has become popular

*For correspondence. (e-mail: jayansurya@yahoo.com)